Transactions, SMiRT-22
San Francisco, California, USA - August 18-23, 2013
Division X

LOCAL BUCKLING OF SC COMPOSITE WALLS AT AMBIENT AND ELEVATED TEMPERATURES

Amit Varma[1], Kai Zhang[2], Sanjeev Malushte[3]

[1] Associate Professor, School of Civil Engineering, Purdue University, West Lafayette, IN
[2] Ph.D. Student, School of Civil Engineering, Purdue University, West Lafayette, IN (kai-zh@purdue.edu)
[3] Bechtel Fellow and Senior Principal Engineer, Bechtel Power Corporation, Frederick, MD

ABSTRACT

This paper presents the results of experimental investigations and finite element analysis of local buckling behavior of the steel faceplates of SC composite walls at ambient and elevated temperatures. This paper is to: (a) establish the slenderness ratio limit of non-slender steel faceplates, (b) investigate the influences of possible accidental thermal loading on the local buckling behavior, and (c) verify that the compressive strength of SC composite walls with non-slender faceplates can be evaluated using design equations in current and proposed design codes at elevated temperature.

INTRODUCTION

The steel faceplates of SC walls serve both as reinforcement and permanent concrete formwork. The steel faceplates may undergo local buckling if the axial compressive stresses are large due to the applied axial loading over the SC wall section. The deformations and locked-in stresses induced in the steel faceplates by concrete casting (i.e. hydrostatic pressure) may also make it more vulnerable to local buckling. Research on local buckling of the steel faceplates of SC walls can be traced back to the 1980's when this type of construction was first used. The SC construction in safety related facilities all over the globe has renewed interest and attention on this issue of plate slenderness and local buckling. This paper presents results of analytical investigations focusing on the behavior and strength of SC walls subjected to compressive loading, and combined axial compression plus thermal loading. The analytical investigations were conducted using nonlinear finite element models (FEM) and analysis approaches that were verified and benchmarked using the experimental database of test results from compressive loading and thermal loading tests.

EXPERIMENTAL DATABASE

Axial Compressive Loading Only

Researchers in Japan and Korea (Akiyama et al., 1991; Usami et al., 1995; Kanchi et al., 1996; Choi and Han, 2009) have experimentally investigated the compressive behavior of SC wall sections. The SC wall specimens were designed with steel faceplates having stud spacing-to-plate thickness (s/t_p) ratio ranging from 20 to 50. Depending on s/t_p ratios, steel faceplates of the SC specimens buckled in plastic, inelastic, and elastic ranges. The steel faceplates buckled outward from the concrete infill between the shear studs. The critical buckling stress could be predicted using Euler's column equation with an effective length coefficient of 0.7, which resembles the pinned-fixed end condition.

This paper evaluated more than 40 test results. Most experiments used a load-unload-reload to failure scheme, albeit the cycle was found to have little effect on initial stiffness and ultimate load. The experimental results from all the tests have been compiled and plotted in Figure 1. The ordinate in the plot is the normalized strain, $\varepsilon_{cr}/\varepsilon_y$, where ε_{cr} is the critical buckling strain of the steel faceplate from compressive tests and ε_y is the nominal yield strain of the steel faceplates. The abscissa is the stud

spacing-to-plate thickness (s/t_p) ratio normalized with respect to the square root of E/F_y, where E is the Young's modulus of steel. Euler's column buckling curve with effective length coefficient (K) equal to 0.7 is also plotted in the figure. It can be observed that the test data points have a trend that follows Euler's curve. Another important observation is that there is no data that falls in the shadowed area where the normalized slenderness ratio is less than 1.0 and ε_{cr} is less than ε_y. This implies that when the normalized plate slenderness ratio [$s/t_p \times \sqrt{F_y/E}$] is less than 1.0, yielding (ε_y) occurs before local buckling (ε_{cr}).

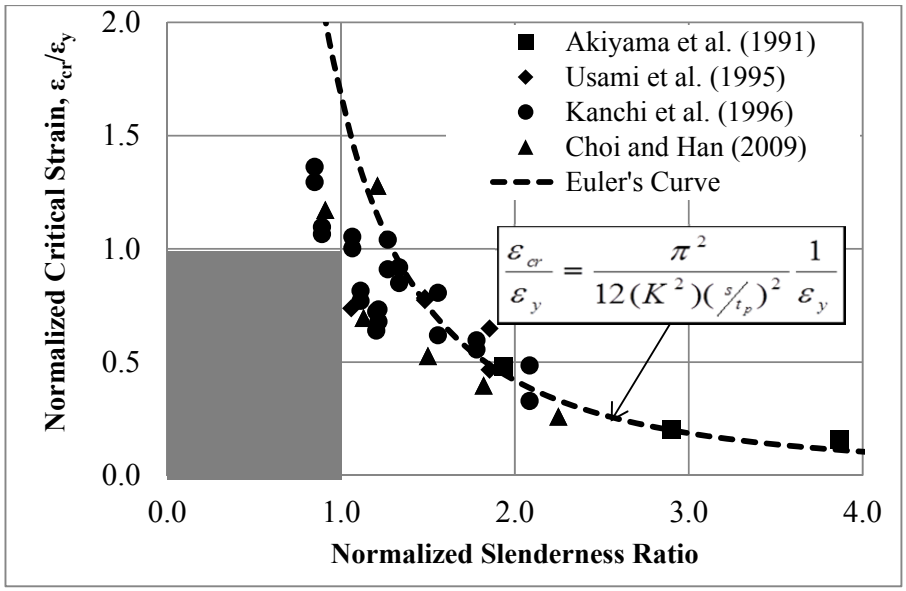

Figure 1. Normalized Critical Strain vs. $s/t_p\sqrt{F_y/E}$ (Experimental Database)

Thermal Loading Only

Sekimoto et al. (2001, 2003) conducted tests to investigate the effects of thermal loading on the concrete cracking and the local buckling of the steel faceplates. The spacing-to-thickness (s/t_p) ratio ranged from 10 to 45. The temperature was increased by 300 °C (572 °F) for all specimens. Most specimens only had concrete cracking because of thermal gradient. Local buckling of the steel faceplate occurred only for the specimen with a spacing-to-thickness (s/t_p) ratio of 45. Three specimens (namely BA, BB and BC) (Sekimoto, 2001) were tested in the restrained thermal loading tests in which the axial deformation was completely restrained from expansion. The steel faceplate thickness was 0.04 inches (4.5 mm) and the spacing-to-thickness (s/t_p) ratios were 12, 18 and 45, respectively. For specimens BA and BB, since no buckling could be observed visually, the temperature was increased by 300 °C (ΔT=300 °C, 572 °F). The buckling of steel faceplate was confirmed visually for specimen BC when the temperature increased by 100 °C (ΔT=100 °C, 212 °F) after which the heating process was terminated. There was neither stud fracture nor pull-out occurred in all the thermal tests.

FINITE ELEMENT MODEL BENCHMARKING

Nonlinear finite element analyses were conducted using ABAQUS (SIMULIA, 2011). There exist different ways to model SC composite walls. One of the approaches is to model every component of SC composite walls as solid elements, i.e. three-dimensional brick elements. In ABAQUS, the C3D8R is a

general-purpose linear brick element with reduced integration and one integration point. Researches (Varma et al., 2012) have proved that the C3D8R element is applicable to model the SC composite walls. In some cases where the meshes are very fine or the structure is very large, the computational time for C3D8R elements becomes considerable. Therefore, another approach is to model different components with alternative elements which can lower the computational cost. For example, the plates can be represented by shell elements (S4R), the shear studs can be modeled with beam elements (B32), and the interface can be modeled with connector elements (CONN3D2). The connector element can employ empirical force-slip relationship developed from pushout tests and thus simulate the interfacial behavior accurately. In this paper, both modeling approaches were benchmarked with test data reported by Kanchi et al. (1996).

Kanchi et al. (1996) performed 11 compression tests on SC walls with plate slenderness ratios ranging from 20 to 50. The C4 series specimens had 0.18-inch (4.5 mm) faceplates with stud spacing-to-plate thickness ratios of 20, 25, 30 and 50. The C6 series consisted of 0.24-inch (6 mm) thick steel faceplates with stud spacing-to-plate thickness ratios of 20, 25, 30, 35 and 40. There were two additional specimens constructed using steel plates with a different strength. The paper included the measured material properties, maximum loads, calculated stiffness, force-displacement curves, and critical buckling strains. Nonlinear finite element analyses were conducted using ABAQUS (SIMULIA, 2011), and the results from solid element models are shown in Figure 2 along with the corresponding experimental results. The dimension of the specimens was 11 inches (280 mm) thick, 39.4 inches (1000 mm) wide and 47.2 inches (1200 mm) high.

In Figure 2, the short straight lines represent the initial stiffness computed as $\sum EA/L$ of the composite section, and reported by Kanchi et al. (1996), where $\sum EA$ is equal to the sum of the steel and concrete elastic modulus and cross-section areas, respectively. As shown, the experimental results were slightly smaller than those predicted by the finite element analyses. This discrepancy is attributed to accidental eccentricities and non-uniform axial loading of the specimens during testing. In general, the results from the finite element analyses compare reasonably with the experimental results.

The 3D nonlinear finite element models were also benchmarked to simulate the restrained thermal tests reported by Sekimoto (2001, 2003). The SC composite walls were modeled using solid eight-node elements (C3D8R) for all the components including the steel faceplates, concrete infill, and the shear studs. The elevated temperature was applied uniformly across the steel faceplate section. The translational degrees of freedom of the four edges of the faceplates were constrained as the boundary condition. The analyses show that no local buckling occurred to the specimens with spacing-to-thickness (s/t_p) ratios of 12 and 18. The model with spacing-to-thickness (s/t_p) ratio of 45 buckled when the temperature increase by about 105 °C (221 °F). The results are shown in Figure 3.

NON-SLENDERNESS LIMIT

The benchmarked finite element models were used to conduct additional parametric studies. The analytical parametric studies were conducted on specimens with normalized s/t_p ratio from 0.8 to 2.5, with the steel faceplate yield stress (F_y) ranging from 36 ksi (248 MPa) to 50 ksi (345 MPa), and concrete compressive strength of 5000 psi (34MPa). The elastic-perfectly plastic stress-strain model was used for steel faceplates. Figure 4 summarizes all the analysis results as a plot of normalized strain ($\varepsilon_{cr}/\varepsilon_y$) versus the normalized plate slenderness ratio $s/t_p \times \sqrt{F_y/E}$. The analysis results shown in Figure 4 are similar to the results from the experimental database shown in Figure 1. The results follow the trends of Euler's column curve. There are not data points within the shadowed region, which implies that when $s/t_p \times \sqrt{F_y/E}$ is less than 1.0, yielding occurs prior to local buckling.

The AISC design philosophy was followed to establish the limiting plate slenderness (s/t_p) ratio for steel faceplates of SC walls. In the AISC Specification (AISC, 2010), compression members are categorized as non-slender or slender. The classification of steel faceplates in SC walls is based on the

stud spacing-to-thickness ratio (s/t_p), defined as the faceplate slenderness ratio. In safety-related facilities such as nuclear power plants, local buckling of steel faceplates is not an acceptable limit state. For axial compression, the steel faceplates are required to have a non-slender section, i.e. undergo yielding prior to local buckling.

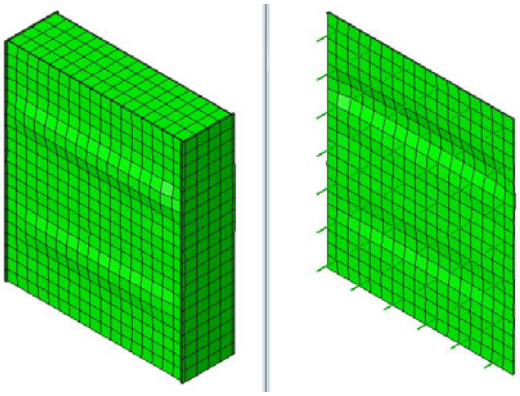

(a) Local Buckling Pattern of C6-30M

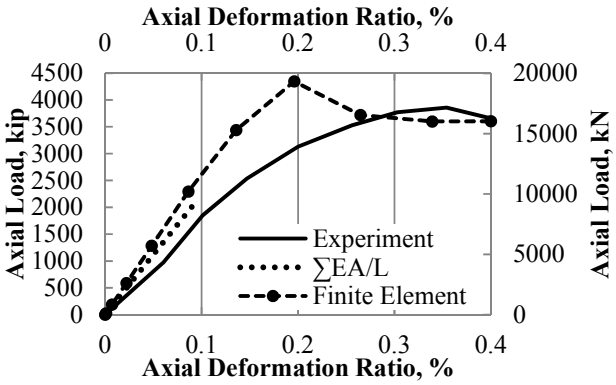

(b) C6-20M Analysis

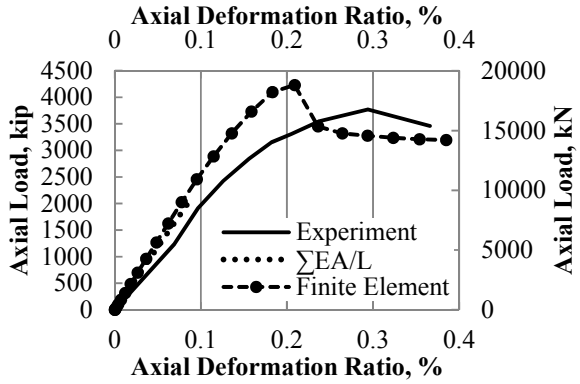

(c) C6-25M Analysis

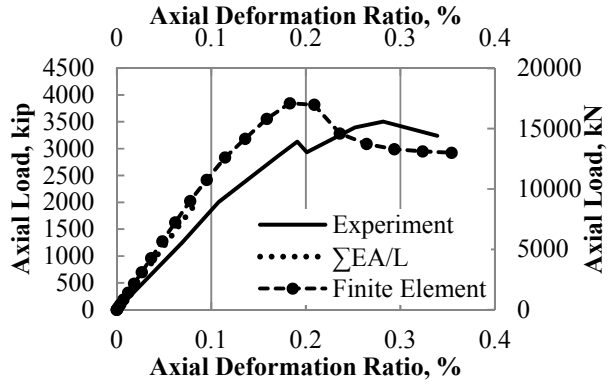

(d) C6-30M Analysis

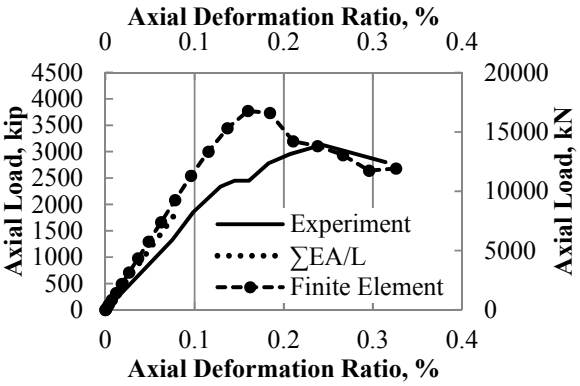

(e) C6-35M Analysis

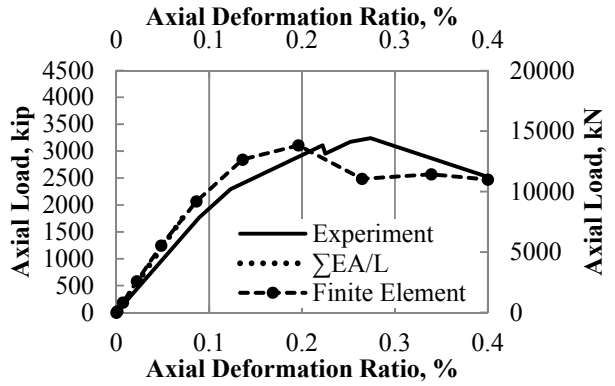

(f) C6-40M Analysis

Figure 2. Finite Element Model Benchmarking with Test Data by Kanchi et al. (1996)

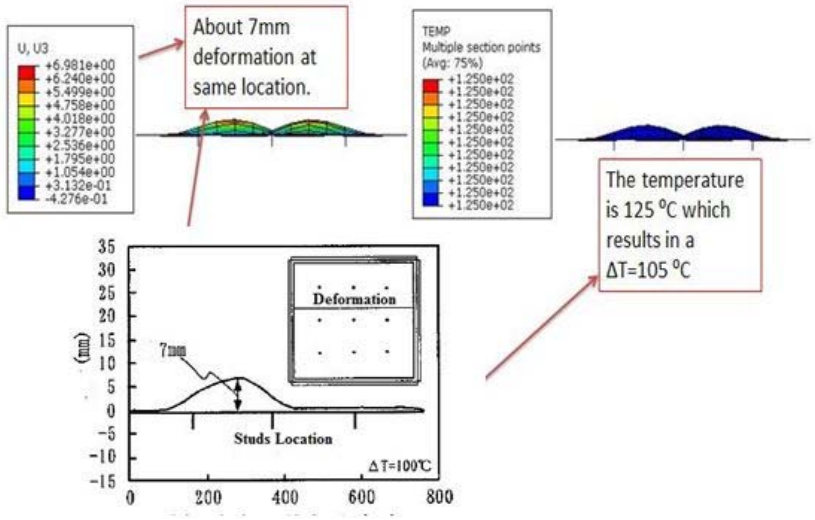

Figure 3. Analysis Results of Restrained Thermal Loading Tests

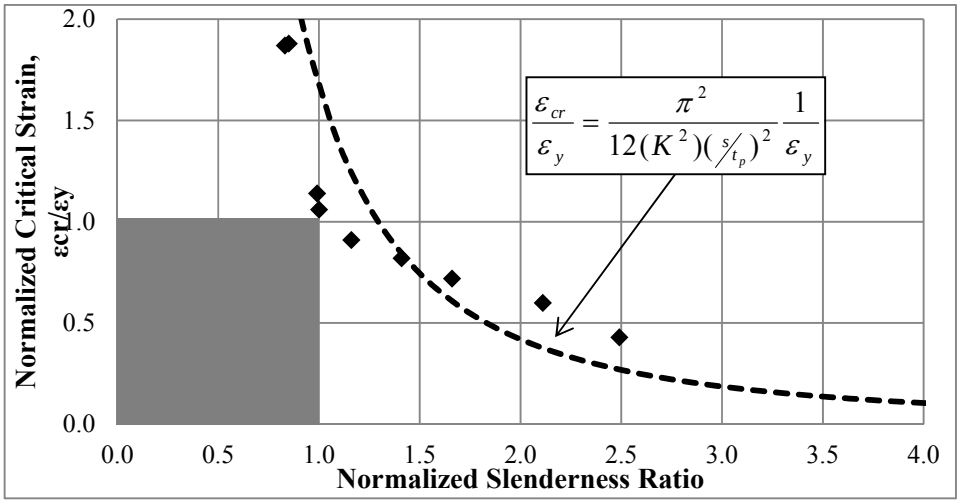

Figure 4. Normalized Critical Strain vs. $s/t_p\sqrt{F_y/E}$ (Finite Element Analysis)

Based on the fact that local buckling does not occur before yielding when the normalized plate slenderness ratio $s/t_p \times \sqrt{F_y/E}$ is less than 1.0, the slenderness limit for a non-slender steel faceplate is proposed to be $s/t_p \le 1.0\sqrt{E/F_y}$.

MODELING OF SC COMPOSITE WALLS UNDER COMBINED LOADING

SC composite walls may be subjected to simultaneous axial loading and elevated temperatures. However, there have been no experimental programs to investigate the behavior of SC composite walls subjected to combined thermal plus compressive loading. In this paper, the benchmarked finite element techniques are used to evaluate the structural performance of SC composite walls for this combined

thermal and compressive loading. The objective of the analyses is to evaluate the effects of elevated temperatures from thermal loading on the axial compressive strength of SC composite walls.

The yield stress (F_y) of the steel faceplates used in the finite element analyses was 57.4 ksi (396 MPa) at ambient temperature. The compressive strength of the concrete infill was 5545 psi (38.2 MPa) at ambient temperature. The stress-strain curves for the steel and the concrete at different temperature magnitudes were generated according to the Eurocode (CEN, 2001). The concrete damage plasticity (CDP) model was used for the concrete and it was assumed that the concrete would crack in tension when the tensile stress was 0.05 times of the compressive strength. The thermal properties of the steel and the concrete, for instance, the thermal capacity and the thermal conductivity, were based on the Eurocode (CEN, 2001) recommendations. Hard, frictionless general contact properties were used in the models to (i) prevent the inter-penetration of the two materials, (ii) allow the interfacial slip and separation, and (iii) allow appropriate heat transfer. The outmost surfaces of the finite element models were heated to a specific temperature in 10 minutes then the temperature was maintained. The output from the heat transfer analysis was stored in a nodal file which was used in subsequent analyses. An eigenvalue analysis was performed on the steel faceplates, and the appropriate eigen-modes were imported as initial geometric imperfection of the faceplates. The stress analysis was executed in two steps. The first step took the temperature distribution and the geometric imperfection to calculate the initial reaction force before the compressive loading was applied. This step calculated stress and strain of the specimen during the heating process. The second step took the results of the first step mentioned above as the initial state, and used the displacement control to monotonically increase the compressive load to failure. The nodal temperature from the heat transfer analysis was imported as the predefine field to represent the sustained heating.

Analysis Parameters

Two parametric studies were performed. The parameter in the first study was spacing-to-thickness ratio (s/t_p), which varied from 20 to 40. The temperature was elevated by 150 °C (302 °F) and was maintained for 30 minutes. The results were compared with the data obtained from the compressive loading tests. The parameter in the second study was the maximum temperature. The finite element models had non-slender steel faceplates. For steel with yield stress of 57.4 ksi (396 MPa), the non-slenderness limit was 22. Therefore, analytical models with spacing-to-thickness (s/t_p) ratios of 10 and 20 were modeled. For each spacing-to-thickness ratio (s/t_p), the temperature magnitude changes were 150 °C (302 °F), 250 °C (482 °F) and 350 °C (662 °F), respectively. The results that will be discussed later show the effect of elevated temperature on the compressive strength of SC composite walls with non-slender faceplate sections.

ANALYSIS RESULTS

Effects of s/t_p Ratio

The analytical models in this study had the same dimension and configurations with the specimens tested by Kanchi et al. (1996). As the aforementioned discussion, the outmost surfaces of the analytical specimens were heated to 170 °C (ΔT=150 °C, 302 °F) assuming the room temperature was 20 °C (68 °F). The heating process finished in 10 minutes and the heat was maintained for 30 minutes. A compressive loading was applied until the analytical specimens failed. Figure 5 shows the analysis load-displacement curves, which are plotted on top of the compressive loading experimental data.

The dash lines with round markers in Figure 5 (a) to (e) are load-displacement curves of finite element analyses. It can be observed that the initial reaction force is non-zero due to the thermal strain induced in the heating process. The solid lines in Figure 5 (a) to (e) are load-displacement curves of the tested specimen under compression. The grey dash lines in Figure 5 (a) to (e) are essentially the experimental data of the compressive specimens, but moved left in the graph to compare with the

analytical results. Table 1 shows the compressive strength of the SC composite walls obtained from the experiments and the finite element analyses. The results from the analyses show little difference on the ultimate capacity as well as the stiffness.

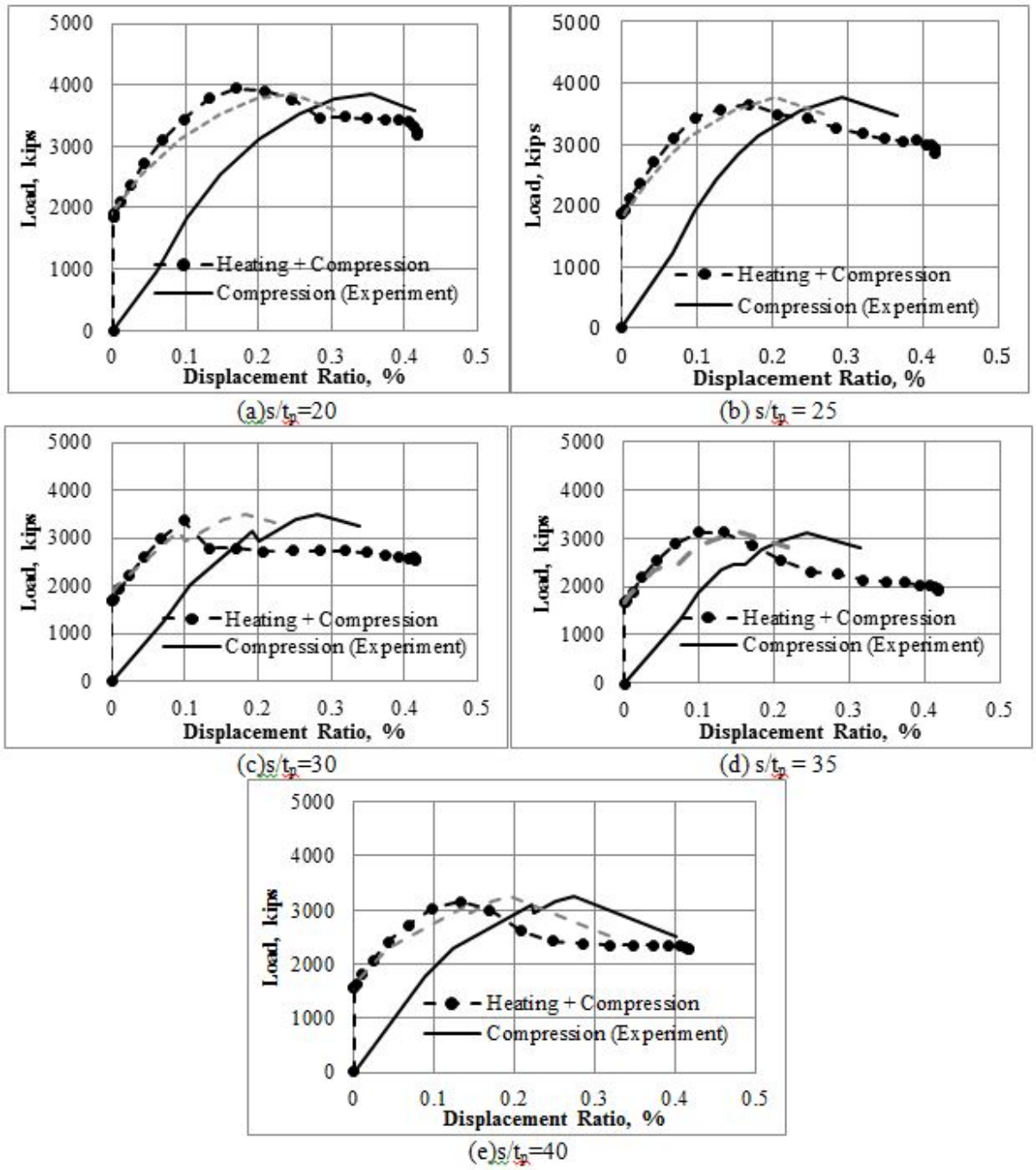

Figure 5. Load-Displacement Curves of Analytical and Experimental Results

Table 1. Comparison of the Compressive Strength

s/t_p	Compressive Strength, kips		
	Exp. (Ambient Temperature)	FEM (Ambient Temperature)	FEM (ΔT=150°C, 302°F)
20	3858	4346	4049
25	3769	4229	3650
30	3505	3845	3370
35	3130	3771	3130
40	3240	3180	3160

Effects of Temperature

Figure 6 shows the analysis results for different temperature magnitudes. The compressive strength of the analytical models has been normalized with respect to the design strength calculated using Equation (1) that will be presented and discussed later. It can be noticed that strength of SC composite walls decreases with the increase of the temperature. Up to 250 °C (482 °F), strength of SC walls predicted using Equation (1) is adequate since the normalized strength is greater than 1. Figure 6 also indicates that strength of SC walls is insensitive to how long they are heated for, by comparing Figure 6 (a) and (c), or Figure 6 (b) and (d).

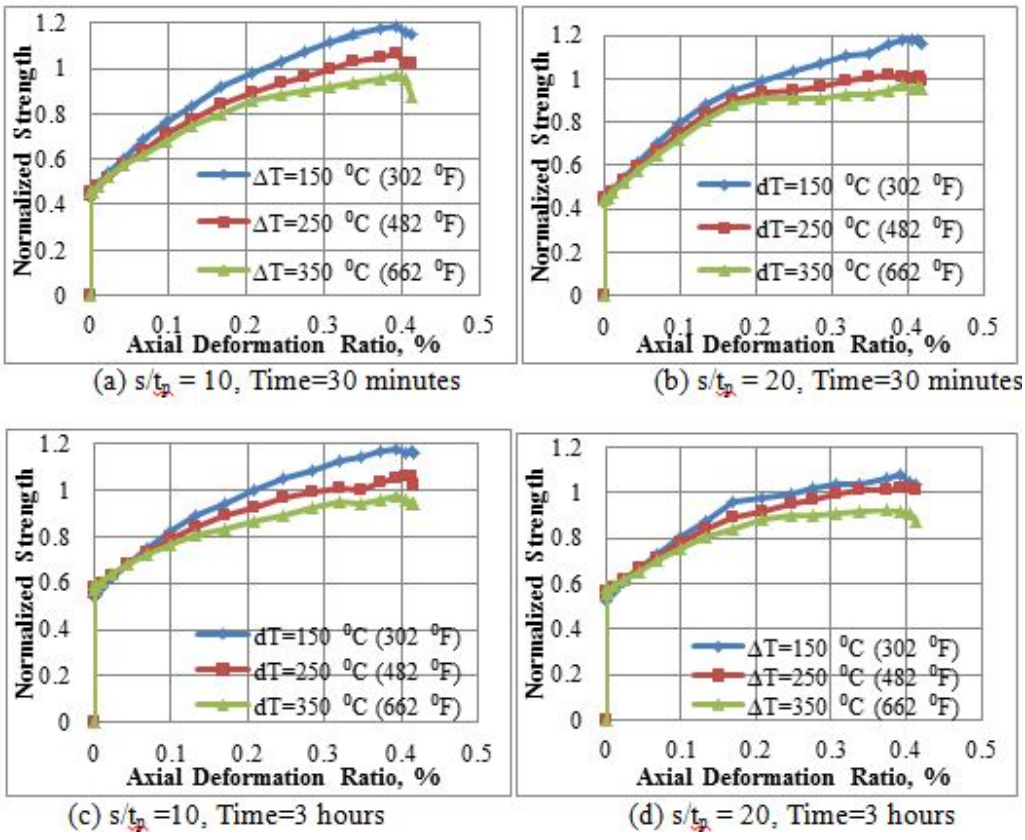

Figure 6. Load-Displacement Curves: Temperature Magnitude as Parameter

DISCUSSIONS

The compressive strength of SC composite walls can be calculated using Equation (1) at ambient temperature, where A_s is the cross-sectional area of one steel faceplate, A_c is the cross-sectional area of the concrete infill, F_y is the yield stress of the steel faceplates, and f'c is the compressive strength of the concrete infill.

$$P_n = 2 \times F_y \times A_s + 0.85 \times f'_c \times A_c \quad (1)$$

The compressive strength of SC composite walls with non-slender faceplates is calculated by Equation (1) and is shown in Table 2. Also shown in Tables 2 is the compressive strength obtained from nonlinear finite element analyses of the same SC composite walls at elevated temperature, and the comparison between the calculated strength. The results indicate that Equation (1) can be used to predict the compressive strength of SC composite walls when the SC section is exposed to an elevated temperature of up to 250 °C (482 °F). When the temperature is higher, for example, ΔT=350 °C (662 °F), Equation (1) becomes a little unconservative, but the overestimation is not significant.

Table 2. Compressive Strength of SC Composite Walls with Non-Slender Steel Faceplates

s/t_p	f'c, ksi	F_y, ksi	Compressive Strength, kip Eq. (1) ①	Compressive Strength, kip, FEM			FEM / Eq.(1)		
				ΔT=150 °C (302 °F) ②	ΔT=250 °C (482 °F) ③	ΔT=350 °C (662 °F) ④	②/①	③/①	④/①
10	5.5	57.4	3448	4100	3661	3355	1.19	1.06	0.97
20	5.5	57.4	3448	4049	3657	3340	1.17	1.06	0.97

The finite element analyses indicate that, compared to the strength at ambient temperature, the compressive strength of SC composite walls with non-slender steel faceplates reduces a little at elevated temperature (Table 1). However, the reduction is insignificant. For SC walls with non-slender steel faceplates, the compressive strength can be calculated using Equation (1) when the temperature is less than 250 °C (482 °F). The analyses also demonstrate that no local buckling occurred on the non-slender steel faceplates, i.e., s/t_p ratio of 10 and 20 in this case, at elevated temperature.

CONCLUSION

- The benchmarked nonlinear finite element modeling techniques can be applied to predict the behavior of SC composite walls under thermal loading, compressive loading, and the combination of the two.
- The steel faceplate must be non-slender for compression. The plate slenderness ratio (s/t_p) -limit established for non-slenderness is based on experimental data and numerical parametric studies conducted using benchmarked finite element analysis models. The faceplate in SC walls must be classified as a non-slender section in order to develop yield stress before local buckling occurs.

- For SC composite walls with non-slender steel faceplates, the compressive strength can be calculated using Equation (1) when the temperature is lower than 250 °C (482 °F). When the temperature is higher, Equation (1) becomes slightly unconservative.
- For non-slender steel faceplates, local buckling of the steel faceplates is not expected to occur for the combined thermal and compressive loadings, and the compressive strength can be calculated using Equation (1).

REFERENCES

American Institute for Steel Construction (AISC), 2010, *Specification for Structural Steel Buildings*, Chicago, Illinois, USA.

Akiyama, H., Sekimoto, H. et al., 1991, "A compression and shear loading tests of concrete filled steel bearing wall", *Transaction of 11th Structural Mechanics in Reactor Technology (SMiRT-11)*, pp. 323-328.

European Committee for Standardisation (CEN), 2001, *Eurocode 1: Actions on Structures, Part 1.2: General Actions – Actions on Structures Exposed to Fire.*

European Committee for Standardisation (CEN), 2001, *Eurocode 4: Design of Composite Steel and Concrete Structures, Part 1.2: Genral Rules – Structural Fire Design.*

Choi, B.J., and Han, H.S., 2009, "An experiment on compressive profile of the unstiffened steel plate-concrete structures under compression loading", *Steel and Composite Structures*, Vol. 9, No. 6, pp. 519-534.

Fukumoto, T., Kato, B., et al., 1987, "Concrete filled steel bearing walls", *IABSE symposium report*, Paris-Versailles, Vol. 55, pp. 467-472.

Kanchi, M., 1996, "Experimental Study on A Concrete Filled Steel Structure Part.2 Compressive Tests (1)" *Summary of technical papers of annual meeting, architectural institute of Japan, Structures*, pp.1071-1072.

Kaneuji, A., Okuda, Y., Hara, K., Masumoto, H., 1989, "Feasibility study of concrete filled steel (SC) structure for reactor building", *Transaction of 10th Structural Mechanics in Reactor Technology (SMiRT-10)*, Anaheim, CA, USA, pp. 67-72.

Miyauchi, Y. et al., 1996, "Experimental Study on a concrete-filled steel structure, Part 3 compressive test (2)", *Summary of technical papers of annual meeting, architectural institute of Japan*, pp.1073-1074.

Sakamoto, M. et al., 1985, "Experimental study on concrete filled steel bearing wall part 2: compression characteristics", *Summary of technical papers of annual meeting, architectural institute of Japan, Structures,* pp.1325-1326.

Sekimoto, H. and Kondo, M., 2001, "Study on property of concrete filled steel bearing wall subjected to high temperature*", Journal of Structural Engineering (Japanese),* Vol. 47B, pp. 481-490.

SIMULIA, 2011, Dassault Systems, Inc., 2011, *Abaqus Analysis User's Manual*, Ver. 6.11

Usami, S., Akiyama, H., Narikawa, M., Hara, K., Takeuchi, M., Sasaki, N., 1995, "Study on a concrete filled steel structure for nuclear plants (part 2). Compressive loading tests on wall members*", Transaction of 13th Structural Mechanics in Reactor Technology (SMiRT-13),* pp. 21-26.

Varma, A.H., Malushte, S.R., Sener, K.C., Booth, P.N., 2012, "Analysis recommendations for steel-composite (SC) walls of safety-related nuclear facilities", *ASCE Structures Congress,* Chicago, IL, USA.

Zhang, K., Varma, A.H., Malushte, S.R., Gallocher, S., 2012, "Effect of Shear Connectors on Local Buckling and Composite Action in Steel Concrete Composite Walls", *submitted to Journal of Nuclear Engineering and Design.*